# X-ray Source Development for High Energy Density Science Using Picosecond Relativistic Laser Interaction with Underdense Plasma

Mitchell Sinclair

University of California, Los Angeles

Los Angeles, California

mdsinclair@ucla.edu

Isabella Pagano
University of Texas at Austin
Austin, Texas

Nuno Lemos

Lawrence Livermore National Laboratory

Livermore, California

Jessica L. Shaw
Laboratory for Laser Energetics
Rochester, New York

Kyle G. Miller

Laboratory for Laser Energetics

Rochester, New York

Adeola Aghedo
Florida A&M University
Tallahassee, Florida

Charles D. Arrowsmith

University of Oxford

Oxford, UK

Paul M. King
University of Texas at Austin
Austin, Texas

Kenneth A. Marsh University of California, Los Angeles Los Angeles, California Co-PI: Félicie Albert

Lawrence Livermore National Laboratory

Livermore, California

PI: Chandrasekhar Joshi University of California, Los Angeles Los Angeles, California

Abstract—We are developing an X-ray source for radiography of high-energy density (HED) experiments by passing a picosecond, relativistic laser beam through an underdense plasma to generate a relativistic beam of electrons. These electrons, in turn, generate bright, (10<sup>10</sup> photon/keV/sr), high energy (10 keV - 1 MeV) X-rays. Over the years, this X-ray platform has been demonstrated on the Titan, Omega EP, and NIF-ARC lasers. This paper gives the present state of the field and argues that the platform has reached a level of maturity where the X-rays produced using this novel platform have the potential to find radiographic applications in a broad range of fields.

Index Terms—X-ray, High Energy Density Science (HEDS), Self-Modulated Plasma Instability, NIF, OMEGA, Backlighter

#### I. Introduction

This platform uses an intense picosecond laser pulse propagating into a gas jet where it excites a multiple period plasma wave in a sub quarter-critical density plasma via the transverse self-modulation instability that is followed by a partially evacuated channel formed by relativistic self-focusing. We have shown that this complex laser-plasma interaction can produce an extremely high charge (10s - 100s nC) relativistic electron beam accelerated by both the longitudinal electric field of the wake and the tightly focused laser pulse as well as the transverse electric field of the laser by a mechanism

This work was performed under the auspices of the U.S. Department of Energy by Lawrence Livermore National Laboratory under Contract DE-AC52-07NA27344. We acknowledge support from the DOE Office of Sciences Early Career Research Program (Fusion Energy Sciences) SCW-1575-1. Work performed by UCLA was supported by DOE grant DE-SC0010064, NNSA grant DE-NA0003873, & NSF Grant No. 2003354. Computational support was provided by NSERC under the m1157 account.

known as direct laser acceleration. We are exploring ways of both increasing the yield as well as the maximum energy of the X-ray photons by increasing the maximum electron energy and the peak electron current. We have used these high charge and energy electron beams to generate X-ray radiation with photon energies exceeding several hundred keV via betatron, inverse Compton scattering, and Bremsstrahlung radiation mechanisms. Current work aims to extend the X-ray energies beyond the MeV energy range and use this platform for radiography of passive and active (HED) targets.

Brilliant, broadband X-ray sources are an important diagnostic tool which can be used for numerous applications. For instance, a beam of few keV X-rays is sufficient to obtain phase contrast images of small features of biological samples [1] whereas tens of keV photons are preferential for characterization of bone microstructures [2]. Higher energy photons (several hundred keV) with a small source size are preferred for diagnosing high-energy density experiments that aim to replicate conditions that exist in the planetary interior in the laboratory [3]. And finally, for radiography of highly compressed capsules in inertial confinement fusion experiments, X-rays with energies on the order of 1 MeV, are needed [4]— [6]. In other words, the goal of this research is to perfect a single platform capable of generating a hyperspectral X-ray source that covers the entire spectral range from a few keV to a few MeV based on a relativistic electron beam generated by the passage of a picosecond (ps) laser beam through an underdense plasma.

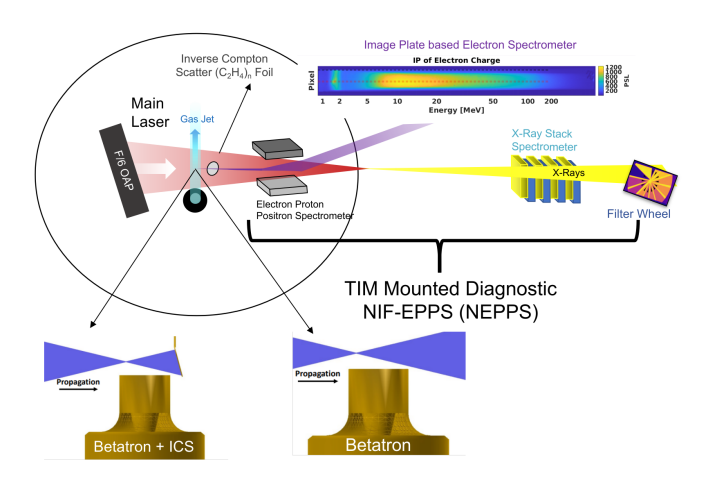


Fig. 1. Layout of the Hyper-Spectral Photon Source Platform & Diagnostics, as applicable to OMEGA\_EP

# II. PHYSICS OF A HYPER-SPECTRAL PHOTON SOURCE

There are numerous methods to produce X-rays, (>150eV photons). Historically the most common method of producing X-rays was by bombarding a high-Z target with a beam of sub 100 keV electrons to generate Bremsstrahlung radiation [7], but today, X-rays are created from relativistic electron beams using undulators and high-Z foils [8], [9]. Other examples include betatron radiation produced by off-axis electrons in both Laser- and Beam- driven Plasma Based Accelerators (PBA) [10]–[12] and up-converting photon energy by colliding a laser pulse with relativistic electrons, Inverse Compton Scattering (ICS) [13]. These techniques all produce quasi-directional X-ray sources which are all founded upon the physical mechanism of synchrotron radiation emission.

The Hyper-Spectral photon source utilizes, betatron, Inverse Compton Scattering (ICS), and Bremsstrahlung radiation from laser-plasma produced relativistic electrons to generate a beam of incoherent but quasi-directional high energy X-rays. This platform has been proven at: the Jupiter Laser Facility, Titan Laser; the Laboratory for Laser Energetics, OMEGA EP; and the National Ignition Facility, Advanced Radiographic Capability Laser. An example of the platform layout at OMEGA EP is shown in Fig. 1.

#### A. The Electron Source

Our hyperspectral X-ray source relies on producing a broad energy spread electron beam by the interaction of a relativistic ps 100 TW-class laser pulse through an underdense plasma. The typical laser intensity is greater than  $10^{19}$  W/cm² and plasma length and density of < 1 cm and >  $10^{18}$  cm³, respectively. The main reason for choosing a ps-class, 1  $\mu$ m laser is that many HED science facilities typically have a multi TW, few nanosecond class lasers as drivers and an accompanying higher laser power, ps class laser as a probe. The interaction of an intense ps laser pulse with an extended plasma is quite complex. The laser intensity is sufficient such that the laser pulse undergoes a longitudinal and transverse self-modulation instability whereby the laser pulse is amplitude modulated

by the electron plasma wave which grows from collective Thomson scattering acting as a noise source over many plasma periods. In addition, if the laser power is above the relativistic critical power for self-focusing,  $P_c=17(\omega_0/\omega_p)^2$  GW, where  $\omega_0$  is the laser radial frequency and  $\omega_{pe}$  is the plasma frequency [14], the plasma electrons can be partially or fully blown out as the laser intensity increases creating a plasma electron density channel. For a plasma density  $n_e$  of  $10^{18}$  cm<sup>-3</sup> and a critical density of  $10^{21}$  cm<sup>-3</sup>, the critical power is typically 17 TW, easily exceeded by the ps-class short pulse lasers accompanying these HEDS facilities.

# B. Electron Generation by Self-Modulation Instabilities & Direct Laser Acceleration

When a laser pulse  $a_0=1$  - 5, where  $a_0$  is the normalized vector potential, propagates through a  $n_e>10^{18}~cm^{-3}$  plasma, the self-modulated instability [1] can modulates the envelope of the laser pulse by the radial transportation of energy. This self-modulated instability can be viewed in 1D as solely due to Forward Stimulated Raman Scattering instability, which must obey the energy and momentum conservation rules given by:

$$\omega_s = \omega_{Laser} \pm m\omega_{pe} \tag{1}$$

$$\vec{k}_s = \vec{k}_{Laser} \pm m\vec{k}_{pe} \tag{2}$$

where  $\omega_s$  ( $\vec{k}_s$ ) is the radial frequency (wave vector) of the forward Raman scattered wave,  $\omega_{Laser}$  ( $\vec{k}_{Laser}$ ) is the lasers radial frequency (wave vector) of the drive laser, and  $\omega_{pe}$  ( $\vec{k}_{pe}$ ) is the plasma frequency (wave vector).

From these equations, one can infer that the beating of the electric fields of the incident laser wave  $\omega_{Laser}$ ,  $k_{Laser}$  and the scattered photons in the exact forward direction  $\omega_s$ ,  $\vec{k}_s$ produces a periodic force on the plasma electrons and produces density fluctuation at  $\omega_{pe}$ ,  $\vec{k}_{pe}$ . The density fluctuations scatter more photons at  $\omega_s$ ,  $\vec{k}_s$  further reinforcing the beat pattern, thus completing a feedback loop. Eventually, the envelope of the incident laser pulse appears to be deeply amplitude modulated at  $k_{pe}$ . Since both the incident and the scattered photons travel at almost c in the underdense plasma, the group velocity of the amplitude modulated envelope also travels near c and, by causality, the phase velocity of the plasma wave  $\omega_{pe}/k_{pe}$  is also close to c. The potential of the growing plasma wave can become large enough and finally trap some of the plasma electrons and accelerate them to energies up to  $4\gamma_{ph}^2=m_ec^2$  where  $\gamma_{ph}=\frac{\omega_0}{\omega_{pe}}$ . Direct Laser Acceleration (DLA) is a second important

Direct Laser Acceleration (DLA) is a second important mechanism present in the SM-LWFA regime, occurring when there is overlap between the incident laser pulse and the plasma electrons [15]–[17]. Usually, this mechanism is explained, in the self-modulation regime, by the interaction of the transverse fields of a long, modulated, laser pulse, with the off-axis electrons' betatron oscillations, providing an acceleration force in the longitudinal direction. Recently, K. Miller has provided theory and simulation insights into DLA [18], which expand upon the experimental and simulation work done by J.

Shaw [19], demonstrating that by de-coupling the longitudinal modes clarifies the contribution to the energy gain of electrons from the transverse laser fields, longitudinal laser field versus the longitudinal wakefield.

#### C. Mechanisms of X-ray generation

Fig. 2 shows a schematic of 3 mechanisms that lead to the generation of directional, hyper-spectral X-rays. These are betatron radiation, inverse Compton scattering and relativistic bremsstrahlung. The reason why the radiation emitted by all three mechanisms can be understood using classical electrodynamics is because the radiated power depends only on the particle's velocity and acceleration in electric and or magnetic fields. We briefly explain these three mechanisms first.

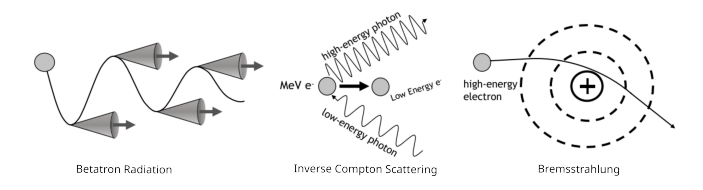


Fig. 2. X-ray Generation Methods: Betatron, Inverse Compton Scattering, & Bremsstrahlung, as employed by the Hyper-Spectral 10 keV - 1 MeV Photon Source.

• Betatron Radiation: is generated whenever the off axis plasma electrons undergo periodic oscillations about the axis of a transverse focusing electric field. This motion is called betatron motion. The transverse electric field in turn is associated with a column of plasma that is either partially or completely void of plasma electrons leaving behind an excess of plasma ions. For electron energies in the 100 MeV range, the betatron oscillation wavelength is on the order few mm. It is well known that when a charged particle is bent (accelerated), in a 1x10<sup>19</sup> cm<sup>-3</sup> plasma ion column, it emits synchrotron radiation. Conceptually, in betatron motion the velocity of the electrons is zero at the top and bottom of their trajectories but the acceleration is maximum, Fig. 2a. It is therefore, at the turning points in their orbits, that the electrons emit radiation most strongly, perpendicular to the acceleration i.e., in the forward direction, and due to the nature of their oscillations, emit radiation in the few keV X-ray range [20].

The betatron radiation particle flux per unit energy per solid angle is characterized by the Bessel function of the 2nd kind,  $K_{2/3}$ , where A is the normalization amplitude, E is the energy range of the emitted photons, and  $E_c = \hbar \omega_c$  is the critical energy of the X-Ray spectrum, where  $\omega_c = 3\gamma^3 c/\rho$  [21].

$$\frac{dI}{dEd\Omega} \propto \frac{A}{E} (\frac{E}{E_c})^2 K_{2/3} (\frac{E}{E_c})^2 \tag{3}$$

• Inverse Compton Scattering: If a photon with energy much less than that of the relativistic electron is inelastically scattered, the scattered photon is frequency

upshifted by the double Doppler effect in a narrow cone of angles in the forward direction, Fig 2b. In our platform, this process can be used to extend the photon energy far beyond that range of the betatron spectrum by reflecting the portion of the incident laser transmitted by the underdense plasma using a low-Z (plastic) material just after the underdense plasma. The transmitted laser light is intense enough to ionize the plastic and turn it into a highly reflecting plasma mirror. Now the collision of the reflected photons with the electrons emanating from the plasma can generate a forward scattered ICS photon beam with a maximum photon energy given by:  $E_{ICS}$  $= \frac{2\gamma^2(1-\cos(\phi))}{1+\gamma^2\theta^2+a_0^2/2+2\gamma k_0\lambda_c} E_{ph}, \text{ where } \gamma \text{ is the relativistic}$  factor of the electron,  $\phi$  is the laser photon angle,  $\theta$  is the scattered X-ray angle,  $a_0$ , is the normalized vector potential of the laser,  $k_0$  is radiation reaction,  $\lambda_c$  is the Compton wavelength, and  $E_{ph}$  is the laser photon energy.

In our experiments we find that the ICS process extends the X-ray spectrum far beyond that produced by betatron radiation and that the experimental X-ray spectra, can be modeled as a sum of exponentials where  $C_i$  is the peak spectral density, and  $E_{T_i}$  is the spectrum temperature [20]

$$\frac{dI}{dEd\Omega} \propto \sum C_i e^{-E/E_{T_i}} \tag{4}$$

Bremsstrahlung: If instead of using a low-Z foil to generate ICS photons one uses a high-Z foil, then the predominant photon generation mechanism is Bremsstrahlung radiation. For instance, using 100 μm to 2 mm high-Z foils, such as Ta & W, electrons can efficiently generate MeV X-rays because strong deflection by the atomic nuclei of the high-Z foil, Fig. 2c. Where E is the photon energy range, B is the peak spectral amplitude, and E<sub>T</sub> is the temperature of the Bremsstrahlung spectrum [20].

$$\frac{dI}{dEd\Omega} \propto Be^{-E/E_T} \tag{5}$$

III. REVIEW OF THE EXPERIMENTS FOR THE DEVELOPMENT OF THE HYPER-SPECTRAL PHOTON SOURCE

In Table I, we summarize the results obtained by the authors in several experimental campaigns on Titan and Omega EP lasers. The Titan laser results were with normalized laser strengths  $a_0=eE/m\omega_0c$  of 2-3 whereas the Omega EP experiments were done with  $a_0=1.6-6.7$ .

#### A. X-ray & Electron Performance Comparison

For X-ray generation, the platform utilizes the intrinsic (to LWFA) betatron radiation process, which has a spectra as described in Eq. 3, with the notable aspect that in the Self-Modulated regime the high charge greatly increases X-ray production [22] where ICS and Bremsstrahlung mechanisms provide mechanisms to create a MeV X-ray sources, which are required by HEDS and high-Z radiographs [23], [24]. It is apparent from the work done by Albert, Lemos, Shaw, and

	OMEGA EP: $a_0 = 1.8 \text{-} 6.7, \tau = 700 \pm 100 \text{ fs},$ $\lambda = 1053 \text{ nm}, f/[10.8,6,5], R(80\%) = 30  \mu\text{m}$	Titan Laser: $a_0 \approx 3, \tau = 700 + 300, -100 \text{ fs}, E = 120 - 150 \text{ J}, \\ \lambda = 1053 \text{ nm}, \text{ w0(86\%)} = 29 \pm 6.1  \mu\text{m}$						
	Shaw [29] 2021 OMEGA EP	King [18] 2019 JLFTitan	Lemos [20] 2019 JLFTitan	Albert [22] 2018 JLFTitan / Callisto	Lemos [25] 2017 JLFTitan	Albert [32] 2017 JLFTitan	Author Year Laser	
	n/a	n/a	10-40 0.3-1.45x10 <sup>12</sup>	10 <sup>11</sup> - 10 <sup>13</sup> 10-40; 10-20	5 x 10° 18 ± 10	0.3-1.45x10 <sup>12</sup>	Yield [Ph/keV/sr] Critical Energy [keV]	
	n/a	n/a	W lmm: $E_c = 1978 \pm 534 \text{ keV}$ Ta l mm: $E_c = 1420 \pm 300 \text{ keV}$ , Poly 100 µm: $E_{T1} = 55 \pm 15 \text{ keV} @ 10-40 \text{ keV}$ $E_{T2} = 100 \pm 20 \text{ keV} @ 80-250 \text{ keV}$	n/a	W Imm: $E_c = 1978 \pm 534 \text{ keV}$ , $B = 0.83 \times 10^9 \text{ [Ph/keV/sr]}$ W 500 $\mu\text{m}$ : $E_c = 838 \pm 111 \text{ keV}$ , $B = 1.4 \times 10^9 \text{ [Ph/keV/sr]}$ Ta 1 mm: $E_c = 1420 \pm 300 \text{ keV}$ , $B = 0.65 \times 10^9 \text{ [Ph/keV/sr]}$	n/a	Brem: $Z$ [mm], $E_c$ [keV], $B$ [Ph/keV/sr] ICS: Material [mm], $E_{\rm TI}$ [keV]	X-Ray Parameters
	n/a	n/a	[1/e²]: 50 μm 100 mrad	100-200 mrad; 10-50 mrad	0.95 mm×1.5 mm 12.4°	- [1/e²] < 35 μm	Source Size Divergence	
	30%, 50%, and 90% 18.5, 25.6, and 85.1 MeV	9.6 <t<sub>1&lt;14.6 MeV 36<t<sub>2&lt;48 MeV; 11<t<sub>1&lt;19 MeV 33<t<sub>2&lt;52 MeV</t<sub></t<sub></t<sub></t<sub>	7 <t<sub>1&lt;18 MeV 20<t<sub>2&lt;50 MeV</t<sub></t<sub>	13 <t<sub>1&lt;18 MeV 20<t<sub>2&lt;50 MeV</t<sub></t<sub>	$T_1 = 7\pm0.06 \text{ MeV}$ $T_2 = 30\pm0.9 \text{ MeV}$	13< T <sub>1</sub> <18 MeV 20< T <sub>2</sub> <50 MeV	Temperature $N_e \propto e^{(-E/T_1)}$	Electron Parameters
	1 - 200 MeV a) 1-188 nC b) 76-695 nC	not listed 1.14 nC > 60 MeV	not listed 4-11 nC > 10 MeV	not listed >100pC	18 - 380 MeV 10.5 nC	not listed	Energy Range Charge	
	[10 mm]: 32 × 39 mrad [6 mm]: R50: 53.9 or 59.4 mrad	0.78 - 1.6; 0.55 - 2.3 $[\theta_{\parallel}/\theta_{\perp}]$ 47 mrad x 27 mrad	100x64 ± 10 mrad	not listed	64x10 mrad	not listed	Divergence Charge	
	Mach 5 2-10 mm	4 mm; 10mm	3-4 mm 500 µm ramps	3 mm 500 μm ramps	4 mm	3 mm	Nozzle	Plasma /
	1.5 - 45	3 - 6.5 0.35 - 0.5	1-15	1 - 15	5	1 - 15	n <sub>e</sub> x10 <sup>18</sup> [cm^-3]	Plasma / Gas Jet Parameters
	He	He	HeN <sub>2</sub> from 1% - 100%	He & HeN <sub>2</sub> from 0% - 100%	Не	He & HeN $_2$ from 0% - 100%	Gas Species	rameters
7.5x1010 [cm-3]	Electron Temperature		Source Size & Divergence /w \( \precedef \) laser polarization Electron Temp [4 mm; 10mm]	X-ray yields @ 10 - 20 keV E <sub>c</sub> of SM; E <sub>c</sub> of Blowout Divergence [SM; Blowout]	X-Ray yield is for Betatron alone		Comments	

 $TABLE\ I$  Summary of X-ray Sources Platform developments as investigated by Albert, Lemos, King, & Shaw and collaborators.

King that combining a high charge X-ray source with ICS and Bremsstrahlung up-converters can boost the critical X-ray energy from approximately 20 keV to 100s - 2000 keV [25]–[28].

For example, Lemos (2018) Table I, demonstrated that Tungsten 1 mm & 500  $\mu$ m and Tantalum 1 mm converters can combine with the betatron radiation source,  $E_c \sim 18~keV$  to create a broadband MeV source with critical energies 0.8, 1.4, & 1.8 MeV [25].

Source size and electron beam divergence are also important quantities for backlighter performance, because in a hypothetical experimental setup, where a gas jet is inserted to radiograph a NIF or OMEGA fusion implosion, propagation distance to a detector is large and the desired features to radiograph are small. A low source size is required for high spatial resolution and a low beam divergence is required to maximize propagation distance to ensure that the bright source illuminates the radiograph target and probes the region of interest.

The articles by Albert, Lemos, King, and Shaw demonstrate the development of this Hyper-Spectral photon source platform. From a high level summary, this platform with its three mechanisms for X-ray production: betatron, ICS, and Bremsstrahlung increase the total flux from the X-ray source and greatly increase the critical X-ray energy. At the JLF, Lemos (2019) [24] demonstrated that the combination of Bremsstrahlung converters greatly impacts the X-ray parameter space, which combined with the new results published by Shaw, (2021) [29] may unveil another discovery by future choices of acceleration length, plasma profile and density and laser focusing geometry to greatly enhance X-ray intensity and critical energy performance. Additionally, because this source is based on a combination effect of laser acceleration and electron converters, (ICS and Bremsstrahlung), there is flexibility to tune this platform for desired applications, for example, spatial resolution versus X-ray energy or X-ray critical energy versus soft X-ray energy intensity [20].

#### IV. CONCLUSION

We have compared the results obtained on two different laser facilities during the course of 6 campaigns that demonstrate that ps, 100 TW class laser pulses propagating through underdense plasmas are capable of producing 10s of nC, ultrarelativistic electron beams. The highest charge of several hundred nC was seen at OMEGA-EP. The electron beams typically have a continuous energy spectra with a maximum energy of between 100-200 MeV. A comparison with experimentally obtained and those observed in PIC simulations suggest that a combination of physical mechanisms are responsible for producing these electrons [18], [30], [31]. These include: both the longitudinal and transverse self-modulation of the laser beam, which generates a relativistic plasma wave; the interaction of the electrons with the transverse field of the laser in the presence of the transverse field of the ions, which leads to periodic oscillation of the electrons; and direct energy gain by the electrons traveling synchronously with the longitudinal field of the focused laser pulse. Where this latter mechanism is a physical description of DLA.

We also have demonstrated that the so-called betatron motion of the electrons in the transverse focusing field of the ions produces oscillatory motion of the electrons about the axis of symmetry that produces forward directed X-rays. The maximum energy of the x-rays can be increased by placing either a low-Z (plastic) or a high-Z foil immediately after the plasma. In the low-Z foil case, a plasma mirror is formed on the foil surface by the laser photons after exiting from the gas jet plasma. Some of these photons are reflected by the plasma mirror and collide with the electron beam producing significantly higher energy forward directed photons (X-rays). Finally, while a higher Z foil also produces ICS radiation, some of it and much of the betatron radiation is attenuated during the passage through the foil. On the other hand, the electron beam, while it impacts the high-Z foil, produces Bremsstrahlung radiation that extends both the yield and maximum energy of the photons to MeV range, suitable for radiographic application. With the inclusion of ICS and Bremsstrahlung converters, there has been the demonstration of exceptionally high temperature X-rays (MeV class) in combination with ICS photons of  $10^{10}$  to  $10^9$  @ 10 - 250  $\frac{Ph}{keV*sr}$  [20], [28], [32].

# A. Future Direction

Next steps for this work includes demonstrating ICS and Bremsstrahlung converters on OMEGA EP, OMEGA, and NIF-ARC, as well as the entire platform on the PETawatt Aquitaine Laser at Laser MegaJoule. These demonstrations will establish the feasibility and reliability of this platform.

The ultimate goal of the platform is to develop an X-ray source capable of producing high-quality radiographs of High Energy Density Science experiments. Applications include radiographing: complex high-Z targets, such as Lead or Tungsten Image Quality Indicators [33]; laser-compressed targets such as Silicon [34] or water [35], to demonstrate spatial-temporal capabilities, and backlighting Inertial Confinement Fusion implosions [4].

## REFERENCES

- [1] S. Fourmaux, S. Corde, K. T. Phuoc, P. Lassonde, G. Lebrun, S. Payeur, F. Martin, S. Sebban, V. Malka, A. Rousse, and J. C. Kieffer, "Single shot phase contrast imaging using laser-produced Betatron x-ray beams," *Optics Letters*, vol. 36, no. 13, pp. 2426–2428, Jul. 2011.
- [2] "Laser-wakefield accelerators as hard x-ray sources for 3D medical imaging of human bone Scientific Reports," https://www.nature.com/articles/srep13244.
- [3] B. A. Remington, "High energy density laboratory astrophysics," *Plasma Physics and Controlled Fusion*, vol. 47, no. 5A, p. A191, Apr. 2005.
- [4] J. Lindl and et. al, "Development of the indirect-drive approach to inertial confinement fusion and the target physics basis for ignition and gain," *Physics of Plasmas*, vol. 2, no. 11, pp. 3933–4024, Nov. 1995.
- [5] H. Abu-Shawareb and e. al.\*, "Lawson Criterion for Ignition Exceeded in an Inertial Fusion Experiment," *Physical Review Letters*, vol. 129, no. 7, p. 075001, Aug. 2022.
- [6] B. Bishop, "National Ignition Facility achieves fusion ignition," https://www.llnl.gov/news/national-ignition-facility-achieves-fusion-ignition, Dec. 2022.

- [7] A. Sommerfeld, "Über die Beugung und Bremsung der Elektronen," Annalen der Physik, vol. 403, no. 3, pp. 257–330, 1931.
- [8] J. D. Jackson, Classical Electrodynamics, 3rd ed. Berkeley: John Wiley & Sons, Inc., 1999.
- [9] V. Zeković, B. Arbutina, A. Dobardžić, and M. Z. Pavlović, "REL-ATIVISTIC NON-THERMAL BREMSSTRAHLUNG RADIATION," International Journal of Modern Physics A, vol. 28, no. 29, p. 1350141, Nov. 2013.
- [10] A. Rousse, K. T. Phuoc, R. Shah, A. Pukhov, E. Lefebvre, V. Malka, S. Kiselev, F. Burgy, J.-P. Rousseau, D. Umstadter, and D. Hulin, "Production of a keV X-Ray Beam from Synchrotron Radiation in Relativistic Laser-Plasma Interaction," *Physical Review Letters*, vol. 93, no. 13, p. 135005, Sep. 2004.
- [11] J. Als-Nielsen and D. McMorrow, Elements of Modern X-ray Physics, 2nd ed. Hoboken: Wiley, 2011.
- [12] S. Wang, C. E. Clayton, B. E. Blue, E. S. Dodd, K. A. Marsh, W. B. Mori, C. Joshi, S. Lee, P. Muggli, T. Katsouleas, F. J. Decker, M. J. Hogan, R. H. Iverson, P. Raimondi, D. Walz, R. Siemann, and R. Assmann, "X-Ray Emission from Betatron Motion in a Plasma Wiggler," *Physical Review Letters*, vol. 88, no. 13, p. 4, 2002.
- [13] K. Ta Phuoc, S. Corde, C. Thaury, V. Malka, A. Tafzi, J. P. Goddet, R. C. Shah, S. Sebban, and A. Rousse, "All-optical Compton gammaray source," *Nature Photonics*, vol. 6, no. 5, pp. 308–311, May 2012.
- [14] E. Esarey, C. B. Schroeder, and W. P. Leemans, "Physics of laser-driven plasma-based electron accelerators," *Reviews of Modern Physics*, vol. 81, no. 3, pp. 1229–1285, 2009.
- [15] A. Pukhov, Z. M. Sheng, and J. Meyer-ter-Vehn, "Particle acceleration in relativistic laser channels," *Physics of Plasmas*, vol. 6, no. 7, pp. 2847–2854, 1999.
- [16] A. Pukhov, "Strong field interaction of laser radiation," 2002.
- [17] T. Wang, V. Khudik, A. Arefiev, and G. Shvets, "Direct laser acceleration of electrons in the plasma bubble by tightly focused laser pulses," *Physics of Plasmas*, vol. 26, no. 8, p. 083101, Aug. 2019.
- [18] P. M. King, K. Miller, N. Lemos, J. L. Shaw, B. F. Kraus, M. Thibodeau, B. M. Hegelich, J. Hinojosa, P. Michel, C. Joshi, K. A. Marsh, W. Mori, A. Pak, A. G. R. Thomas, and F. Albert, "Predominant Contribution of Direct Laser Acceleration to High-Energy Electron Spectra in a Low-Density Self-Modulated Laser Wakefield Accelerator," *Physical Review Accelerators and Beams*, vol. 24, no. 1, p. 11302, 2020.
- [19] J. L. Shaw, N. Lemos, L. D. Amorim, N. Vafaei-Najafabadi, K. A. Marsh, F. S. Tsung, W. B. Mori, and C. Joshi, "Role of Direct Laser Acceleration of Electrons in a Laser Wakefield Accelerator with Ionization Injection," *Physical Review Letters*, vol. 118, no. 6, pp. 1–5, 2017.
- [20] N. Lemos, P. King, J. L. Shaw, A. L. Milder, K. A. Marsh, A. Pak, B. B. Pollock, C. Goyon, W. Schumaker, A. M. Saunders, D. Papp, R. Polanek, J. E. Ralph, J. Park, R. Tommasini, G. J. Williams, H. Chen, F. V. Hartemann, S. Q. Wu, S. H. Glenzer, B. M. Hegelich, J. Moody, P. Michel, C. Joshi, and F. Albert, "X-ray sources using a picosecond laser driven plasma accelerator," *Physics of Plasmas*, vol. 26, no. 8, p. 083110, Aug. 2019.
- [21] F. Albert, B. B. Pollock, J. Shaw, K. A. Marsh, Y.-H. Chen, D. Alessi, J. E. Ralph, P. A. Michel, A. Pak, C. E. Clayton, S. H. Glenzer, and C. Joshi, "Betatron x-ray production in mixed gases," in *Betatron X-Ray Production in Mixed Gases*, vol. 8779. SPIE, May 2013, pp. 258–266.
- [22] F. Albert, N. Lemos, J. L. Shaw, P. M. King, B. B. Pollock, C. Goyon, W. Schumaker, A. M. Saunders, K. A. Marsh, A. Pak, J. E. Ralph, J. L. Martins, L. D. Amorim, R. W. Falcone, S. H. Glenzer, J. D. Moody, and C. Joshi, "Betatron x-ray radiation from laser-plasma accelerators driven by femtosecond and picosecond laser systems," *Physics of Plasmas*, vol. 25, no. 5, p. 056706, May 2018.
- [23] C. Courtois, R. Edwards, A. Compant La Fontaine, C. Aedy, S. Bazzoli, J. L. Bourgade, J. Gazave, J. M. Lagrange, O. Landoas, L. L. Dain, D. Mastrosimone, N. Pichoff, G. Pien, and C. Stoeckl, "Characterisation of a MeV Bremsstrahlung x-ray source produced from a high intensity laser for high areal density object radiography," *Physics of Plasmas*, vol. 20, no. 8, p. 083114, 2013.
- [24] M. D. Perry, J. A. Sefcik, T. Cowan, S. Hatchett, A. Hunt, M. Moran, D. Pennington, R. Snavely, and S. C. Wilks, "Hard x-ray production from high intensity laser solid interactions (invited)," *Review of Scientific Instruments*, vol. 70, no. 1, pp. 265–269, Jan. 1999.
- [25] N. Lemos, F. Albert, J. L. Shaw, D. Papp, R. Polanek, P. King, A. L. Milder, K. A. Marsh, A. Pak, B. B. Pollock, B. M. Hegelich, J. D. Moody, J. Park, R. Tommasini, G. J. Williams, H. Chen, and

- C. Joshi, "Bremsstrahlung hard x-ray source driven by an electron beam from a self-modulated laser wakefield accelerator," *Plasma Physics and Controlled Fusion*, vol. 60, no. 5, p. 054008, May 2018.
- [26] F. Albert, B. B. Pollock, J. Shaw, K. A. Marsh, J. E. Ralph, A. Pak, C. E. Clayton, S. H. Glenzer, and C. Joshi, "Betatron radiation from laser plasma accelerators," in *Laser Acceleration of Electrons, Protons,* and Ions III; and Medical Applications of Laser-Generated Beams of Particles III, vol. 9514. SPIE, May 2015, pp. 72–81.
- [27] P. M. King, N. Lemos, J. L. Shaw, A. L. Milder, K. A. Marsh, A. Pak, B. M. Hegelich, P. Michel, J. Moody, C. Joshi, and F. Albert, "X-ray analysis methods for sources from self-modulated laser wakefield acceleration driven by picosecond lasers," *Review of Scientific Instruments*, vol. 90, no. 3, p. 033503, Mar. 2019.
- [28] F. Albert, N. Lemos, P. King, J. L. Shaw, A. L. Milder, C. Goyon, D. Kalantar, B. Remington, N. Ose, D. Alessi, M. Prantil, K. A. Marsh, B. B. Pollock, A. Pak, A. Saunders, F. V. Hartemann, S. S. Q. Wu, R. Falcone, B. Hegelich, J. D. Moody, S. H. Glenzer, P. Michel, and C. Joshi, "X-ray Sources from Self-modulated Laser Wakefield Acceleration: Applications in High Energy Density Sciences," in OSA High-brightness Sources and Light-driven Interactions Congress 2020 (EUVXRAY, HILAS, MICS). Washington, DC: Optica Publishing Group, 2020, p. ETh5A.2.
- [29] J. L. Shaw, M. A. Romo-Gonzalez, N. Lemos, P. M. King, G. Bruhaug, K. G. Miller, C. Dorrer, B. Kruschwitz, L. Waxer, G. J. Williams, M. V. Ambat, M. M. McKie, M. D. Sinclair, W. B. Mori, C. Joshi, H. Chen, J. P. Palastro, F. Albert, and D. H. Froula, "Microcoulomb (0.7 ± 0.4/0.2 μC) laser plasma accelerator on OMEGA EP," Scientific Reports, vol. 11, no. 1, p. 7498, Dec. 2021.
- [30] N. Lemos, K. A. Marsh, B. B. Pollock, F. S. Tsung, F. Albert, C. Joshi, J. L. Shaw, and J. L. Martins, "Self-modulated laser wakefield accelerators as x-ray sources," *Plasma Physics and Controlled Fusion*, vol. 58, no. 3, p. 034018, 2016.
- [31] J. L. Shaw, "Direct Laser Acceleration in Laser Wakefield Accelerators," Disertation, UCLA, Los Angeles, CA, 2016.
- [32] F. Albert, N. Lemos, J. L. Shaw, B. B. Pollock, C. Goyon, W. Schumaker, A. M. Saunders, K. A. Marsh, A. Pak, J. E. Ralph, J. L. Martins, L. D. Amorim, R. W. Falcone, S. H. Glenzer, J. D. Moody, and C. Joshi, "Observation of Betatron X-Ray Radiation in a Self-Modulated Laser Wakefield Accelerator Driven with Picosecond Laser Pulses," *Physical Review Letters*, vol. 118, no. 13, p. 134801, Mar. 2017.
- [33] F. Albert and A. G. R. Thomas, "Applications of laser wakefield accelerator-based light sources," *Plasma Physics and Controlled Fusion*, vol. 58, no. 10, p. 103001, Nov. 2016.
- [34] J. C. Wood, D. J. Chapman, K. Poder, N. C. Lopes, M. E. Rutherford, T. G. White, F. Albert, K. T. Behm, N. Booth, J. S. Bryant, P. S. Foster, S. Glenzer, E. Hill, K. Krushelnick, Z. Najmudin, B. B. Pollock, S. Rose, W. Schumaker, R. H. Scott, M. Sherlock, A. G. Thomas, Z. Zhao, D. E. Eakins, and S. P. Mangles, "Ultrafast Imaging of Laser Driven Shock Waves using Betatron X-rays from a Laser Wakefield Accelerator," Scientific Reports, vol. 8, no. 1, pp. 1–10, 2018.
- [35] M. Balcazar, Mario, T. Ostemayr, H.-E. Tsai, P. Campbel, S. Hakimi, R. Jacob, Y. Ma, R. Young, P. King, R. Simpson, E. Grace, B. Kettle, E. E. Los, F. Albert, J. van Tilborg, S. P. Mangles, J. Nees, E. H. Esarey, C. Geddes, A. G. Thoms, and C. C. Kuranz, "Dynamic X-ray imaging of shock evolution and plasma instability formation using a laser wakefield accelerator," in *Bulletin of the American Physical Society*. American Physical Society, 2022.